

A New Fault-Tolerant Control of Wind Turbine Pitch System Based on ANN Model and Robust and Optimal Development of MRAC Method

M. Kamarzarrin¹; M. H. Refan^{2,*}; A. Dameshghi³

1- Faculty of Electrical Engineering, Shahid Rajaee Teacher Training University, Tehran, Iran, Email: kamarzarrin.mehrnoosh@sru.ac.ir

2- Faculty of Electrical Engineering, Shahid Rajaee Teacher Training University, Tehran, Iran, Email: Refan@sru.ac.ir

3- Faculty of Electrical Engineering, Shahid Rajaee Teacher Training University, Tehran, Iran, Email: a.dameshghi@sru.ac.ir

*Corresponding author

Received: 2020-01-18

Revised: 2020-04-24

Accepted: 2020-09-16

Abstract: In this paper, a new method is provided for Fault-Tolerant Control (FTC) of wind turbine pitch systems. One of the common faults in wind turbines is the defects of the pitch sub-system. Each blade of wind turbines tracks a reference signal; it is generated by the main controller unit, defects of actuators, or disturbance decrease of the reference signal quality. Classic controllers cannot deal with the disturbance and compensate for the faults to maintain system performance in normal operating conditions. For this purpose, a novel method based on Optimal Robust Model Reference Adaptive Control (ORMRAC) is presented, the output of the proposed method is a new adaptive rule. The ORMRAC method is robust, optimal, and fast at the same time. The proposed structure includes Fault Detection (FD) and FTC units. FD acts based on the generation and evaluation of residuals. The residual generation is based on Artificial Neural Network (ANN) model. When there is disturbance or fault in the pitch system and residual exceeds the certain threshold, the FT unit is activated. The proposed FT method is tested and evaluated using a wind turbine simulator based on practical data. The results indicated the proper performance of the proposed method in comparison with conventional MRAC and some other methods.

Keywords: Pitch angle, wind turbine (WT), MRAC, ORMRAC, fault tolerant, ANN.

1. Introduction

Energy is one of the major challenges of the industry in the world. Quality, reliability, and renewability of energy are important [1, 2]. Wind turbine (WT) as one of the converters of mechanical energy to electrical energy is susceptible to various faults [3]. Fault Detection (FD), diagnosis, and process modification are essential to increase the reliability and availability of wind turbines [4]. When there is a fault, there should be a strategy to compensate the current condition [5]. The control subsystem should be able to compensate the system faults. These classes of control systems are known as Fault-Tolerant Control (FTC) [6]. After fault isolation, the system must continue to operate in the presence of a fault [7-8]. FTC strategy increases the power generation and prevents the down-time of WTs [9]. Disturbances are due to increases of wind speed, dynamic and transient conditions of WT. On the other hand, in electrical pitch system fault occurs in actuators [10]. Fault and disturbance lead to inaccuracies in the setting pitch angle [11].

Several methods have been proposed for robust control of the pitch subsystem of WT. Based on the linear matrix inequality approach [12], a comprehensive way of applying the H₂ planning theory is proposed for power regulation via a pitch controller. As [13-15], predictive and robust control is used to pitch control. A robust observer along with a control strategy based on sliding mode is used for control of the WT in [15]. The L₁ output feedback controller is used to design the controller and reduce the load of the controller in [16]. Ref [17] introduced a MIMO controlling strategy based on the H_∞ norm for WT. Many articles are provided regarding the WT pitch controller with the FTC ability. In [18] a Reference Model Adaptive Control (MRAC) method combined with Neural Network (NN) is presented. An observer-based control system is designed for sensor fault in [19]. Ref [20] presented a Linear Parameter-Varying (LPV) control system for WT at maximum power and under the influence of a fault in the pitch system. In [21], a fuzzy approach is provided to identify and control WT. Another fuzzy method is introduced in [22, 23]. The main idea of the [24] is the use of MRAC to adjust the generator

torque. This controller presented an appropriate response under the disturbance, uncertainty of the model, and actuator fault. Ref [25] is FD and FTC of WTs via a discrete-time controller with a disturbance compensator. An active FTC approach to an offshore WT model is presented in [26]. A FTC controller based on the virtual sensor is designed to manage the faulty WT pitch system before maintenance is conducted; A fault detection algorithm based on the Kalman filter is designed [27]. A model-based method for FTC of Pitch of an Offshore WT [28]. A method is proposed for fault-tolerant individual pitch control of WT with actuator faults. The proposed scheme consists of a collective pitch control augmented with individual pitch control, and a fault detection and diagnosis system [29]. An adaptive sliding observer is proposed to estimate parametric pitch actuator faults [30]. FTC structure in [30] includes a baseline PI control with fault estimation and compensation. Another sliding mode FTC method is examined based on the 5MW NREL wind turbine system [31].

In this paper, a new structure is proposed to prevent the parameter changes around the reference points. The proposed FTC method is based on Optimal Robust Model Reference Adaptive Control (ORMRAC). A good FTC must be active and should provide an appropriate response to faults with changes in the control structure. The method presented in this paper performs FT without prior knowledge of the fault, uncertainties, and disturbance of the model. For this purpose, a simulator based on 2.5 MW of MAPNA WT is used. Commercial WT uses a PI controller for the pitch system. Upon the occurrence of the fault or in case of disturbance, the FTC unit is activated. In this paper, a data-based residual generation and evaluation method are used for the diagnosis of actuators based on the Artificial Neural Network (ANN) model. The proposed system shifts from PI control mode to FTC mode if the difference between the measured values in WT exceeds the value modeled with ANN.

The contribution of this paper as follows:

- A new control method of wind turbines based on Robust and Optimal development of RMAC is presented.
- A new adaptive law and the new cost function is defined.
- The proposed method is used for the FTC of the wind turbine.
- The proof and analysis stability of the proposed method is done based on the Lyapunov theory.
- The fault of wind turbine pitch-blade detects by ANN is based on residual generation.
- The new FTC method was tested by practical data of 2.5 MW wind turbine based on simulator setup.

The paper is organized as follows: In the second part, the proposed FTC method is described. The third part of the article is the WT simulator and section four describes the proposed structure used for the FTC. The simulation results of the FTC proposed method are presented in section five. The implementation of the proposed structure is section 6. Finally, the last part of the article is the conclusions.

2. The Fault-Tolerant Control method: Optimal Robust Reference Model Adaptive Control (ORMRAC)

The proposed FTC method is based on the MRAC and MRAC is one of the most important adaptive control methods. Fig. 1 shows a block diagram of classical MRAC. In [32, 33], it is shown that this controller will be stable in the absence of disturbance. Despite the advantages of adaptive control, there are challenges for the implementation of this type of controller in systems with high reliability and sensitivity [34-36]. Normally, there is a balance between stability and tracking performance. Fast adaptation improves the tracking performance, but due to low robustness, it may negatively affect the stability of the control system [35]. σ -modification [37] and e -modification [34] are two robust adaptive rules. According to the 18th theory of chapter 4 of [38], MRAC is not robust in limited disturbances and actuator fault [34-37]. The method presented in this paper is based on the optimization of error function $e(t)$ and adaptive loop transfer function. Based on the structure of the adaptive reference model in Fig.1, several objectives followed [34, 39]: Objective 1: designing a controller where $y(t)$ asymptotically follows $r(t)$ and while maintaining the reference model stability margin in the presence of disturbance, fault, and uncertainty. Objective 2: maintaining system stability margin. Objective 3: While maintaining stability, system performance should not be diminished.

The system is as Eq.1:

$$\dot{x}(t) = Ax(t) + B[u(t) + f(x(t))], \quad x(0) = x_0, \quad t \geq 0 \quad (1)$$

Where $x(t): [0, \infty) \rightarrow \mathbb{R}^n$ is a state vector, $u(t): [0, \infty) \rightarrow \mathbb{R}^p$ is control vector, $A \in \mathbb{R}^{n \times n}$ and $B \in \mathbb{R}^{n \times p}$ are known so that (A, B) is controllable and $f(x(t)): \mathbb{R}^n \rightarrow \mathbb{R}^p$ is the disturbance, uncertainty, actuator fault, or the sum of them for the system.

The reference model system is intended as Eq.2.

$$\dot{x}_m(t) = A_m x_m(t) + B_m r(t), \quad x_m(0) = x_{m0}, \quad t \geq 0 \quad (2)$$

Where $x_m(t) \in \mathbb{R}^n$ and $t \geq 0$ are reference state vectors and $r(t) \in \mathbb{R}^r$ is the command vector. $A_m \in \mathbb{R}^{n \times n}$ is Hurwitz matrix and $B_m \in \mathbb{R}^{n \times r}$. Adapted actuator fault function (disturbance) parametrically is linear in accordance with the Eq. 3.

$$f(x(t)) = \Theta^{*T} \Phi(x(t)) + \varepsilon(x(t)) \quad (3)$$

Where $\Theta^* \in \mathbb{R}^{m \times p}$ is unknown constant ideal weight matrix and $\Phi: \mathbb{R} \rightarrow \mathbb{R}^m$ is regression function that is defined as $\Phi(x) = [\Phi_1(x), \Phi_2(x), \dots, \Phi_m(x)]$. $\varepsilon(x(t)): \mathbb{R}^n \rightarrow \mathbb{R}^p$ is an approximation error.

Here, the aim is to determine the feedback control rule $u(t): [0, \infty)$, so that the dynamic system state and nonlinear uncertainties in the Eq.1 asymptotically follow the reference model state of Eq.2. In the following, the control rule is considered as Eq.4. [37, 38].

$$u(t) = u_n(t) - u_{ad}(t), \quad t \geq 0 \quad (4)$$

Where nominal control rule $u_n(t), t \geq 0$ is defined as Eq.5.

$$u_n(t) = -K_x x(t) + K_r r(t), \quad t \geq 0 \quad (5)$$

Where $r(t) \rightarrow \mathbb{R}^p \in \mathcal{L}_\infty$ is the command vector and $r(t) \rightarrow \mathbb{R}^p \in \mathcal{L}_\infty$ is the stable gain matrix and $A - BK_x$ is

the Hurwitz matrix. $K_r \in \mathbb{R}^{p \times p}$ is the gain matrix of $r(t)$ and $u_{ad}(t) \in \mathbb{R}^p$ is a direct adaptive signal that estimates the parametric uncertainty of the system and is defined as Eq.6.

$$u_{ad}(t) = \Theta^T(t)\Phi(x(t)), \quad t \geq 0 \quad (6)$$

Where $\Theta(t) \in \mathbb{R}^{m \times p}$ is an estimate of the unknown parameters that satisfies Θ^* , also, $A_m = A - BK_x$ and $B_m = BK_r$.

$$\dot{\Theta} = \Gamma\Phi(x(t))e^T(t)PB \quad (7)$$

Where $\Gamma \in \mathbb{R}^{m \times m}$ is positive definite matrix and $e(t) \triangleq x(t) - x_m(t)$, $t \geq 0$ is fault state of system and $P \in \mathbb{R}^{n \times n}$ is a positive definite solution of the Lyapunov Eq.8.

$$A_m^T P + PA_m + R = 0 \quad (8)$$

Where $R \in \mathbb{R}^{n \times n}$ is a positive definite matrix and A_m is Hurwitz that follows the convergence theory of Lyapunov, and $P \in \mathbb{R}^{n \times n}$ is unique positive definite that satisfies Eq.8 despite $R \in \mathbb{R}^{n \times n}$ positive definite matrix. Given the assumption 1, Eq. 9 is true.

$$|f(x(t)) - \Theta^T(t)\Phi(x(t))| < \epsilon(x), \quad \epsilon(x) < \bar{\epsilon} \quad (9)$$

In following the ORMRAC method will be explained. The new adaptive rule is based on minimizing the tracking error and adaptive loop function.

a. Tracking error function

A part of minimizing is tracking error function and \mathcal{L}_2 norm related to $e(t)$. If we consider as estimation error of the parametric uncertainty and tracking error definition is as $e(t) = x_m(t) - x(t)$ the tracking error function will be the difference between to equation of (1) and (2) as the following Eq.10.

$$\dot{e}(t) = A_m e(t) + B[\tilde{\Theta}^T(t)\Phi(x(t)) - \epsilon(x(t))] \quad (10)$$

b. Adaptive loop transform feature

While for tracking error we need the stability analysis of Lyapunov for evaluation of the performance of a nonlinear system, addressing the stability merging needs linearity. Regarding this problem, adaptive control formulated in the previous section, due to linearization leads to adaptive Eq.5. Fig. 2 shows the result of this linearization with respect to fixed weight (update process is not considered) [36]. When $f(x(t)) = 0$, the upper bound of this structure represents the closed-loop system without uncertainties. Calculated margin with a broken loop in the red zone with $\tilde{\Theta}$ in Fig.2 is in accordance with a margin of reference model (fixed and constant). The lower part of this figure shows the adaptive control effect (steady-state) on the properties of the reference model loop. However, this is not common and in fact, the weight of the reference model changes, but if it is fixed and even if $e(t) = 0$, it is clear that the reference model stability margin is not maintained. The stability margin of the reference model is ensured by the feedback block at the bottom of Fig. 2. In this paper, in addition to minimizing the tracking error, minimization of $\Theta^T(t)\frac{d\Phi(x(t))}{dx}$ is a purpose. It is assumed that $\frac{d\Phi^T(x(t))}{dx}$ has full rank.

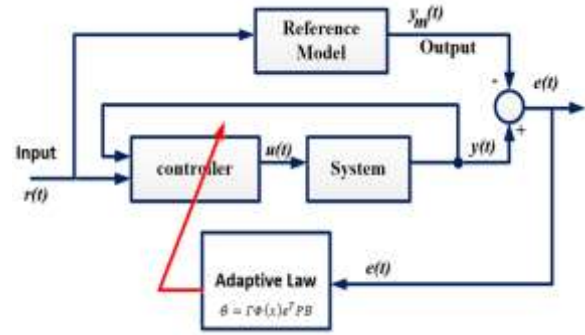


Fig. 1. Structure of a conventional MRAC

The new Robust Adaptive Control method is expressed in according to the adaptive rule of Eq.11 to modify the MRAC in the presence of disturbance and fault.

$$\begin{aligned} \dot{\Theta}(t) = & -\Gamma\Phi(x(t)) \left[e^T(t)P - \right. \\ & \left. \xi \frac{d\Phi^T(x(t))}{dx} \Theta(t) A_m^T Q \right] B \end{aligned} \quad (11)$$

The aim is to obtain a robust optimal adaptive rule. To prove the robust optimal adaptive rule in Eq. 11, the minimization of the second norm of cost function Eq.12 will be addressed.

$$\begin{aligned} J = \lim_{t \rightarrow \infty} \frac{1}{2} \int_0^{t_f} & \left[e(t) - \Delta(t) \right]^T Q \left[e(t) - \Delta(t) \right] + \\ & \left[\frac{d\Phi^T(x(t))}{dx} \Theta(t) \right]^T G \left[\frac{d\Phi^T(x(t))}{dx} \Theta(t) \right] dt \end{aligned} \quad (12)$$

Where Δ is expressing the lower bound of tracking error, $Q = Q^T > 0 \in \mathbb{R}^{n \times n}$ and $G = G^T > 0 \in \mathbb{R}^{n \times n}$ are weight matrixes and $\Gamma = \Gamma^T > 0 \in \mathbb{R}^{m \times m}$ is an adaptive gain matrix, $\xi > 0 \in \mathbb{R}$ is modification parameter and $P = P^T > 0 \in \mathbb{R}^{n \times n}$ is the result of the Lyapunov function of Eq. 13.

$$\begin{aligned} PA_m + A_m^T P &= -Q \\ PA_m + A_m^T P &= -G \end{aligned} \quad (13)$$

For optimal solve of cost function Eq.12, this problem can be formulated using Pontryagin's minimum principle and the Hamiltonian equation will be as Eq.14.

$$\begin{aligned} H &= \frac{1}{2} \left[e(t) - \Delta(t) \right]^T Q \left[e(t) - \Delta(t) \right] \\ &+ \frac{1}{2} \left[\frac{d\Phi^T(x(t))}{dx} \Theta(t) \right]^T G \left[\frac{d\Phi^T(x(t))}{dx} \Theta(t) \right] \\ &+ p^T(t) \left[A_m e(t) + B \tilde{\Theta}^T(t) \Phi(x(t)) - B \epsilon(x(t)) \right] \end{aligned} \quad (14)$$

Where $p(t): [0, \infty) \rightarrow \mathbb{R}^n$ is auxiliary variable and prerequisite for solving Pontryagin is expressed as the Eq. 15.

$$\begin{aligned} \dot{p}(t) = & -\nabla H_e^T - \nabla H_{\frac{d\Phi^T(x(t))}{dx} \Theta}^T = -Q \left[e(t) - \right. \\ & \left. \Delta(t) \right] - G \left[\frac{d\Phi^T(x(t))}{dx} \Theta(t) \right] - A_m^T p(t) \end{aligned} \quad (15)$$

Where $p(t_f \rightarrow \infty)$ value is considered to be zero, because $e(0)$ value of is known. When $\Theta^T(t)\Phi(x(t))$ is considered as a control variable, the optimal condition is expressed as Eq.16.

$$\nabla H_{\tilde{\Theta}^T \Phi} = p^T(t)B \quad (16)$$

And control rule can be formulated as Eq.17 using gradient update rule.

$$\begin{aligned} \dot{\tilde{\theta}}(t) &= -\Gamma \nabla H_{\tilde{\theta}^T} = -\Gamma \Phi(x(t)) \nabla H_{\tilde{\theta}^T \Phi} \\ &= -\Gamma \Phi(x(t)) p^T(t) B \end{aligned} \quad (17)$$

Approximate solution of $p(t)$ can be obtained by sweep method [39, 40] and considering $p(t)$ as $W(t)e(t) + R(t) \frac{d\Phi^T(x(t))}{dx} \theta(t)$, where $(t): [0, \infty) \rightarrow$

$$\begin{aligned} \dot{W}(t)e(t) + W(t)[A_m e(t) + B\theta^T \Phi(x(t)) - B\theta^{*T} \Phi(x(t)) - B\varepsilon(x(t))] + \dot{R}(t) \frac{d\Phi^T(x(t))}{dx} \theta(t) + \\ R(t) \frac{d\left(\frac{d\Phi^T(x(t))}{dx} \theta(t)\right)}{dt} = -Q[e(t) - \Delta(t)] - A_m^T \left[W(t)e(t) + R(t) \frac{d\Phi^T(x(t))}{dx} \theta(t) \right] - G \frac{d\Phi^T(x(t))}{dx} \theta(t) \end{aligned} \quad (18)$$

$$\dot{W}(t) + W(t)A_m + A_m^T W(t) + Q = 0 \quad (19)$$

$$\dot{R}(t) - G - A_m^T R(t) = 0 \quad (20)$$

$$-Q\Delta(t) + R(t) \frac{d\left(\frac{d\Phi^T(x(t))}{dx} \theta(t)\right)}{dt} +$$

$$W(t)B[\theta^T \Phi(x(t)) - \theta^{*T} \Phi(x(t)) + \varepsilon(x(t))] = 0 \quad (21)$$

It can be seen that Eq. 20 has a unique and stable solution at $\tau = t_f - t$ [41].

$$-\frac{dW(\tau)}{d\tau} + W(\tau)A_m \quad (22)$$

$$+ A_m^T W(\tau) + Q = 0$$

$$-\frac{dR(\tau)}{d\tau} + A_m^T R(\tau) + G = 0 \quad (23)$$

If the initial time conditions are as $W(0) = 0$ and $R(0) = 0$ then the uniqueness of the solution of the Lyapunov differential equation is visible from Eq.22. Infinite-time horizon solutions $W(\tau)$ and $R(\tau)$ tend to a constant value. Considering $W(\tau) \rightarrow P$, $R(\tau) \rightarrow S$ and $\tau \rightarrow \infty$ and equations (24) and (25), $p(t)$ the value will be defined as Eq.26.

$$PA_m + A_m^T P = -Q \quad (24)$$

$$S = -A_m^{-T} G \quad (25)$$

$$p(t) = Pe(t) - A_m^{-T} G \frac{d\Phi^T(x(t))}{dx} \theta(t) \quad (26)$$

Then, the optimal solution with a unique adaptive rule is expressed as Eq.27.

$$\begin{aligned} \dot{\theta}(t) &= -\Gamma \Phi(x(t)) \left[e^T(t)P - \right. \\ &\left. \theta^T(t) \frac{d\Phi(x(t))}{dx} G^T A_m^{-1} \right] B \end{aligned} \quad (27)$$

In the proposed method, the optimal solution will lead to the new robust adaptive rule. The performance and robustness are two important factors in the controller design and generally, in control system design, we need to create a balance between robustness and performance of the system. So to implement the adaptive rule, which adjustable for optimal use, the correction parameter $\xi > 0$ is introduced. If the tracking performance is higher than the robust stability, ξ value will be limited to a small amount. In the case of limitations and when $\xi = 0$, MRAC is standard, MRAC achieves asymptotic tracking performance, but it sacrifices the robust stability. In other words, if the robust stability is a priority in the design, then ξ values should be large to make a balance between performance and robust stability. Then, S will be as Eq.28.

$$S = -\xi A_m^{-T} G \quad (28)$$

And the value of $p(t)$ will be considered as Eq. 29.

$R^{n \times n}$ and $R(t): [0, \infty) \rightarrow R^{n \times n}$ are matrixes of effective functions. By differentiation of sides of the recent equation, we would have Eq. 18. If $W(t_f \rightarrow \infty) = 0$ and $R(t_f \rightarrow \infty) = 0$ then the solution of Eq. 18 will be expressed as equations (19)-(21).

$$p(t) = Pe(t) - \xi A_m^{-T} G \frac{d\Phi^T(x(t))}{dx} \theta(t) \quad (29)$$

Then the control rule Eq.27 will be as Eq.30. Assuming $t_f \rightarrow \infty$ bounds of $\Delta(t)$ will be calculated according to Eq.30.

$$\begin{aligned} \|\Delta(t)\| &\leq \|Q^{-1}\| \left[\xi \|A_m^{-T} G\| \left\| \frac{d\left(\frac{d\Phi^T(x(t))}{dx} \theta(t)\right)}{dt} \right\| + \right. \\ &\left. \|PB\| \|f(x(t))\| \right] \end{aligned} \quad (30)$$

Where Eq.30 depends on modification parameter ξ and adaptive uncertainty $\|f(x(t))\|$. As long as there is uncertainty, $\|\Delta(t)\|$ will be limited and error tracking is carried out asymptotically in MRAC, but there is a cost for stability. To prove the stability of the proposed adaptive rule, using the theory of Lyapunov, Lyapunov function $V(t)$ will be considered as Eq.31.

$$V(t) = e^T(t)Pe(t) + \text{trace} \left(\tilde{\theta}^T(t) \Gamma^{-1} \tilde{\theta}(t) \right) \quad (31)$$

Where $V(t)$ was zero at the point of balance and is a positive function. According to the Lyapunov theorem for the stability of the system, the energy of the system should be downtrend; in other words, the result of it derivative is negative. To evaluate the derivative of Eq.31 and for some simplifications:

$$\begin{aligned} \dot{V}(t) &= \left(A_m e(t) + B \left[\tilde{\theta}^T \left(\Phi(x(t)) \right) - \right. \right. \\ &\left. \left. \varepsilon(x(t)) \right] \right) e^T(t)P + e^T(t)P \left(A_m e(t) + \right. \\ &\left. B \left[\tilde{\theta}^T \left(\Phi(x(t)) \right) - \varepsilon(x(t)) \right] \right) + \end{aligned} \quad (32)$$

$$\begin{aligned} &\text{trace} \left(\dot{\tilde{\theta}}^T(t) \tilde{\theta}^T(t) \Gamma^{-T} + \tilde{\theta}^T(t) \Gamma^{-1} \dot{\tilde{\theta}}(t) \right) \\ \dot{V}(t) &= e^T(t) (A_m^T P + PA_m) e(t) + \\ &2e^T(t)PB \left[\tilde{\theta}^T \left(\Phi(x(t)) \right) - \varepsilon(x(t)) \right] + \\ &\text{trace} \left(-\Gamma \Phi(x(t)) \left[e^T(t)P - \right. \right. \\ &\left. \left. \xi \theta^T(t) \frac{d\Phi(x(t))}{dx} G^T A_m^{-1} \right] B + \tilde{\theta}^T(t) \Gamma^{-T} + \right. \end{aligned} \quad (33)$$

$$\begin{aligned} &\left. \tilde{\theta}^T(t) \Gamma^{-1} \left[-\Gamma \Phi(x(t)) \left[e^T(t)P - \right. \right. \right. \\ &\left. \left. \xi \theta^T(t) \frac{d\Phi(x(t))}{dx} G^T A_m^{-1} \right] B \right) \\ \dot{V}(t) &= e^T(t) (-Q) e(t) + \\ &2e^T(t)PB \left[\tilde{\theta}^T \left(\Phi(x(t)) \right) - \varepsilon(x(t)) \right] - \end{aligned} \quad (34)$$

$$\begin{aligned} &2\text{trace} \left(\tilde{\theta}^T(t) \Phi(x(t)) \left[e^T(t)P - \right. \right. \\ &\left. \left. \xi \theta^T(t) \frac{d\Phi(x(t))}{dx} G^T A_m^{-1} \right] B \right) \\ \text{Or each row vector such as } &A = \\ [a_1 \dots a_i \dots a_n] \in R^n &\text{ and } B = \end{aligned}$$

$[b_1 \dots b_i \dots b_n] \in R^n$ matrix trace will be expressed as $\text{trace}(A^T B) = BA^T = \sum_{i=1}^n a_i b_i$. So $\dot{V}(t)$ of Eq.34 can be expressed as Eq.35.

$$\begin{aligned} \dot{V}(t) = & -e^T(t)Qe(t) + \\ & 2e^T(t)PB \left[\tilde{\theta}^T(\Phi(x(t))) - \varepsilon(x(t)) \right] - \\ & 2e^T(t)PB\tilde{\theta}^T(t)\Phi(x(t)) + \\ & 2\xi \tilde{\theta}^T(t) \frac{d\Phi(x(t))}{dx} G^T A_m^{-1} \end{aligned} \quad (35)$$

After some simplification on the recent equation, $\dot{V}(t)$ will be as Eq.36.

$$\begin{aligned} \dot{V}(t) = & -e^T(t)Qe(t) + \\ & 2e^T(t)PB\tilde{\theta}^T(\Phi(x(t))) - 2e^T(t)PB\varepsilon(x(t)) - \\ & 2e^T(t)PB\tilde{\theta}^T(t)\Phi(x(t)) + \\ & 2\xi \underbrace{\tilde{\theta}^T}_{\tilde{\theta} - \theta_0^*}(t) \frac{d\Phi(x(t))}{dx} (t) A_m^{-T} Q B \end{aligned} \quad (36)$$

$$\begin{aligned} \dot{V}(t) = & -e^T(t)Qe(t) - 2e^T(t)PB\varepsilon(x(t)) + \\ & 2\xi \tilde{\theta}^T(t) \frac{d\Phi(x(t))}{dx} G^T A_m^{-1} B - \\ & 2\xi \theta_0^* \frac{d\Phi(x(t))}{dx} G^T A_m^{-1} B \end{aligned} \quad (37)$$

The derivative can be limited as Eq.38 by considering the extremes of values.

$$\begin{aligned} \dot{V}(t) \leq & -\|e(t)\|[\lambda_{\min}(Q)\|e(t)\| - 2\|PB\|\varepsilon_0] + \\ & 2\xi \left\| \frac{d\Phi(x(t))}{dx} \right\| \lambda_{\min}(G^T A_m^{-1} B) [\|\tilde{\theta}(t)\| - \|\theta_0^*\|] \end{aligned} \quad (38)$$

By calculating the squares, $\dot{V}(t)$ can be expressed as Eq.39.

$$\dot{V}(t) \leq -c_1[\|e(t)\| - c_2]^2 + c_3[\|\tilde{\theta}(t)\| - c_4]^2 + c_5 \quad (39)$$

Where $c_1 \triangleq \lambda_{\min}(Q)$, $c_2 \triangleq \|PB\| \varepsilon_0 / \lambda_{\min}(Q)$, $c_3 \triangleq \xi \left\| \frac{d\Phi(x(t))}{dx} \right\| \lambda_{\min}(G^T A_m^{-1} B)$, $c_4 \triangleq \theta_0^*$ and $c_5 \triangleq c_1 c_2^2 + c_3 c_4^2$.

Then it will be considered as Eq.40.

$$B_r = \left\{ (e(t), \tilde{\theta}(t)) \in R^n \times R^{m \times p} : c_1[\|e(t)\| - c_2]^2 + c_3[\|\tilde{\theta}(t)\| - c_4]^2 \leq c_5 \right\} \quad (40)$$

Considering the limit as Eq.40, it can be seen that $\dot{V}(t)$ is positive inside and negative outside. As a result, outside this area, V is a decreasing function. $(e(0), \tilde{\theta}(0))$ is limited all the times and $e(t)$ will be limited after $t > T$.

Since $\|e(t)\| \geq r$ and $\left\| \frac{d\Phi(x(t))}{dx} \right\| \geq k$ and according to Eq. 41 where $r = c_2 + \sqrt{c_5/c_1}$ and $\kappa = c_4 + \sqrt{c_5/c_3}$ the adaptive rule is stable outside B_r . In other words, $\dot{V}(t) \leq 0$. By defining $q(t) = [e^T(t), \tilde{\theta}^T(t)]^T$ and $B_r =$

$\{q(t) : \|q(t)\| < \rho\}$ where is a large enough range and assuming a limited error corresponding to $\tilde{\theta}$ as $\|\tilde{\theta}\| \leq \theta_0^*$, then the most limited set is defined as Eq.41. The bounds of tracking error and ranges used to prove stability are shown in Fig. 3.

$$\rho = \sqrt{\frac{\lambda_{\max}(P)r^2 + \lambda_{\max}(\Gamma^{-1})\kappa^2}{\lambda_{\min}(P)}} \quad (41)$$

Where $\bar{P} = \text{diag}[P, \Gamma^{-1}]$. To prove this range, Ω_α and α considered as $\Omega_\alpha = \{q(t) \in B_r : q^T(t)\bar{P}q(t) \leq \alpha\}$ and $\alpha = \min_{\|q(t)\|=r} q^T(t)\bar{P}q(t) = r^2 \lambda_{\min}(\bar{P})$.

Since $V(t)$ is defined as $V(t) = q^T(t)\bar{P}q(t) = e^T(t)Pe(t) + \text{trace}[\tilde{\theta}^T \Gamma^{-1} \tilde{\theta}]$ and Ω_α is an invariant set with the length of $\alpha \geq \lambda_{\max}(P)r^2 + \lambda_{\max}(\Gamma^{-1})\kappa^2$ then the least size of B_r is estimated by Eq. 41. The transient operation of ORMRAC depends on modification parameters ξ and adaptive gain Γ . This is similar to the transient operation of σ and e , which depend on σ and $\sigma\|e\|$. Increasing the value of these parameters in any robust adaptive control rule will lead to a reduced transient operation. So in the case of ORMRAC transient operation and robust stability simultaneously improved. This is possible by improving adaptive gain and proper selection of the ξ parameter. When Γ Gain increases, MRAC tracking improves, but at the same time stability faces challenges against un-modeled dynamic. So when uncertainty is high and there are disturbances and we need fast adaptation and improving the gain as well, MRAC will not be able to maintain the stability, while ORMRAC in fast adaptation will have a good robust stability. In addition, in the proposed method with a minimizing the condition of adaptive loop transmission $\frac{d\Phi^T(x(t))}{dx} \tilde{\theta}(t)$, the problems raised in this case such as controller design where $y(t)$ asymptotically follows $r(t)$ and reference model margin stability is preserved in the presence and in the absence of disturbance, will be solved.

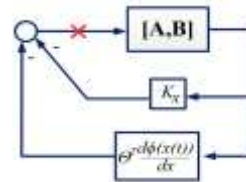


Fig. 2. Linear adaptive system

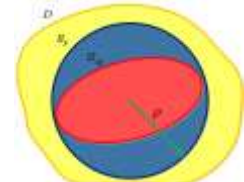


Fig. 3. Tracking error bounds

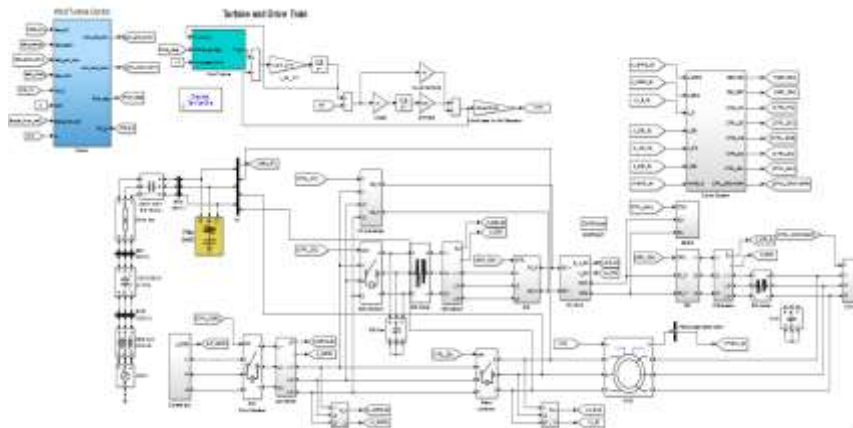


Fig. 4. Overall schematic of the simulator

Table I. Characteristics of the 2.5 MW MAPNA WT

WT		DFIG	
Wind speed	11.43 m/s	Rated Power	2.5 MW
Power Coefficient	0.43	Number of poles	Three pairs of poles
Air density	1.225 Kg/m ³	Speed	75.-1310 u/min(50 HZ)
Turbine blade radius	53m	Stator rated voltage	690V
Tip speed ratio	9	Armature resistance	0.0014 ohm
Blade surface	8495	Rated frequency	50 Hz
Start generation	3.5/4 m/s	Stator Resistance	0.0014 ohm
Stop generation	25 m/s	Rotor Resistance	0.0014 ohm
Gearbox	Gear with 3 stage by 1:79.6	Stator leakage inductance	9.8e-5 H
Back to Back converter		Rotor leakage inductance	8.6e-5 H
Switching Frequency of Rotor	2.5 KHz	Magnetizing inductance	0.00169 H
Switching Frequency of Stator	3 KHz	Stator/Rotor turns ratio	0.3
DC-link Capacitor/ DC-link Voltage	22 mF/1100 v	Line resistance	0.0001 ohm

3. Simulation Setup for the WT system

The model of commercial turbines implemented in this setup and partial data is used for input of this setup. The developed model is a 2.5 MW turbine based on DFIG and real data of wind farm owned by MAPNA used as input of setup [42]. The wind farm includes 13 turbines, wind turbines are active in 3.6 to 25 meters per second of wind speed, and wind speed increases up to 32 meters per second as well. MATLAB/SIMULINK is used for modelling. Fig. 4 is a general schematic of the simulator. The general features of WT are in accordance with Table I. The developed model is a 2.5 MW turbine based on DFIG and actual data of wind farm owned by MAPNA is used as input of setup [42]. The generator has six poles, and as can be seen in Fig. 4, it is connected to the grid via an AC-DC-AC converter. A vector control strategy is applied to the back-to-back converter. For the rotor side converter and grid side converter, a technique is employed based on Space Vector Modulation (SVM) with stator Field Oriented Control (FOC) strategy and Grid Voltage Oriented Control (GOC), respectively.

WT pitch subsystem is divided into two categories, hydraulic and electric. The hydraulic actuator changes the angle of the blades through a hydraulic system. In this study, the WT uses an electrical pitch system. Servomotor regulates the blade pitch angle based on set points received from the main control system, the three actuators, three engines, and three PLCs work together to regulate the pitch angle.

WT consists of various subsystems that all parts need to be modeled; in this section, the modeling of the pitch sub-system is presented. At speeds less than the nominal speed, there is no need to use blade pitch control and pitch angle is about zero degrees. In the case of variable speed turbine blade pitch adjustment, the maximum pitch angle of the blades (β_{max}) is 90 degrees. The block diagram of the pitch control second-order model is shown in Fig. 5. Blade angle β should follow the reference blade angle β_{cmd} . The second order transfer function is following Eq.42:

$$\ddot{\beta}(t) + 2\xi\omega_n\dot{\beta}(t) + \omega_n^2\beta(t) = \omega_n^2u(t) \quad (42)$$

Where ω_n and ξ are natural frequency and damping coefficient and for less fault status these values for WT in our study are 9.6 and 0.63, respectively.

4. The proposed structure

The proposed structure for WT actuator fault-tolerant control is composed of 4 units. The proposed structure is shown in Fig. 6.

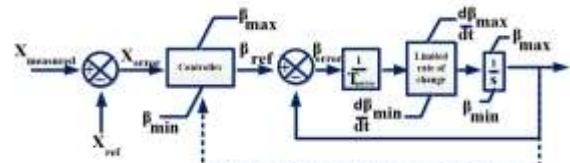


Fig. 5. Block diagram of blade-pitch control

4.1. Residual Generation Unit

There are different methods to generate residuals. Two main methods are known as model-based and data-driven methods, in model-based methods the difference between the measured values of plant and the signal of a mathematical model of that plant is the "residual" and then residual evaluation is done for FD process. Due to the lack of accurate mathematical models in this article, the identification method such as ANN is used to identify plants.

4.2. Fault Detection Unit

Each FT system requires a FD section. When a fault (disturbance) signal is higher than the threshold, the FT subsystem tries to compensate the fault by changing the control structure and keeps the system performance at the optimal level. FD has two healthy and non-healthy modes, the amount of residual is involved in triggering a switch (threshold is 0.5), and this switch is determining sign between normal and the fault modes.

4.3. Fault-Tolerant Control Unit

The structure of this unit based on a graphic structure is shown at the bottom of Fig. 6. If the switch function is activated, it means that there is a fault in the pitch system, in this state determining the pitch angle is based on ORMRAC to compensate of the faults.

4.4. Pitch control unit based on PI

PI is the internal controller of WT for the pitch subsystem. In normal operating conditions of pitch subsystem (without disturbance or actuator fault), the PI controller applies the desirable blade pitch angle. The operation of this unit is so that it receives rotor speed as the input and compares it with the reference value and resulting is the error, this error goes to pitch model (Fig. 5).

Using a PI pitch controller the desired angle is adjusted.

5. Evaluation and simulation of the proposed structure

This section includes the evaluation of the proposed structural main blocks including PI controller, residual generator, FD unit, and FT unit.

5.1. Use of the PI controller without fault

This general equation of the PI controller is as follows:

$$u(t) = K_p \left[e(t) + \frac{1}{K_I} \int e(\tau) d\tau \right] \quad (43)$$

Where $u(t)$ is the input signal and $e(t)$ is the error signal and is determined as the difference between the output signal and the reference signal, $e(t) = y(t) - r(t)$.

To design the PI controller, a linear form of the nonlinear system should be obtained. Accordingly, we rewrite the equations of the system and then a function of the input to output is obtained and then $\omega_r = 17.1$ rpm, $v = 12.43 \frac{m}{s}$, $\beta = 0.01$ deg and yaw fix error is linearized using the Jacobian matrix. Linearized aerodynamic equations of WT are as equations 44 and 45.

$$\begin{bmatrix} \dot{\omega}_r \\ \dot{\beta} \end{bmatrix} = \begin{bmatrix} \delta & \gamma \\ 0 & -\frac{1}{T_\beta} \end{bmatrix} \begin{bmatrix} \omega_r \\ \beta \end{bmatrix} + \begin{bmatrix} 0 \\ \frac{1}{T_\beta} \end{bmatrix} \beta_{cmd} \quad (44)$$

$$\omega_r = [1 \quad 0] \begin{bmatrix} \omega_r \\ \beta \end{bmatrix} \quad (45)$$

By placement of studied turbine parameters, ω_r to β_{cmd} the transform function is as Eq.46.

$$TF(s) = \frac{2012}{s^2 + 74.79s + 1096} \quad (46)$$

The transform function obtained in Eq.46 is a minimum phase with a relative degree of 2. Considering the response of the open-loop of the linear system, the coefficients ΔM , L_r and R_r can be determined.

The process response speed is $R_r = 10.8$, lead-phase is $L_r = 0.5$ and the difference between horizontal asymptotes of process time response is $\Delta M = 64$.

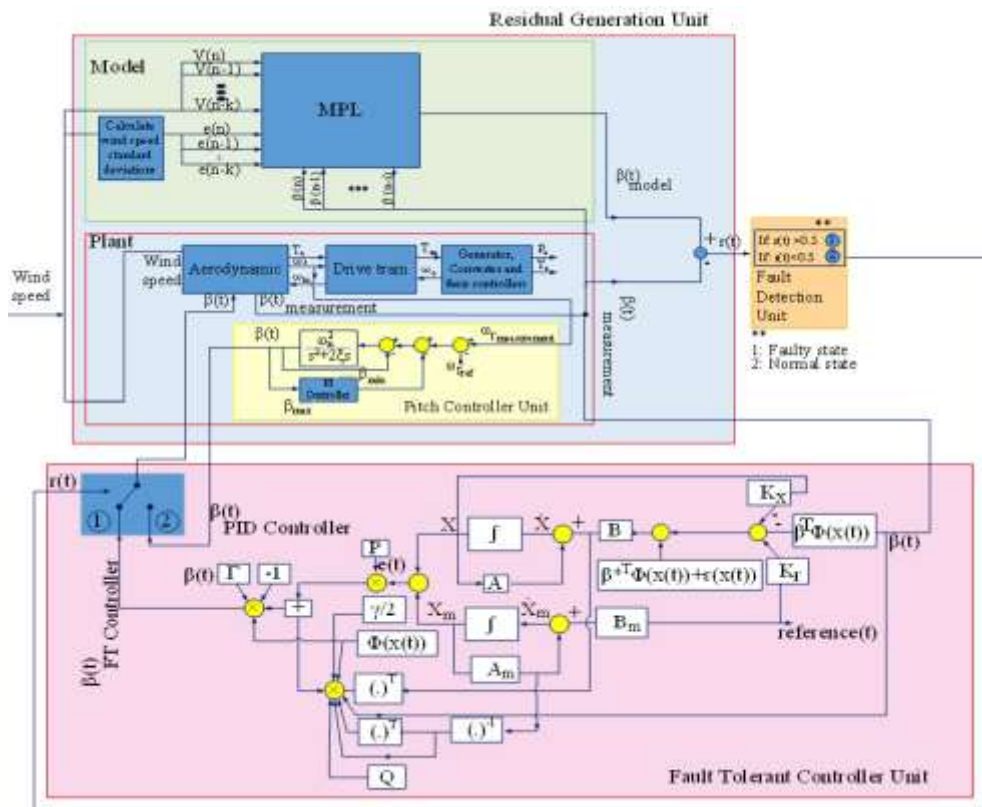


Fig. 6. The proposed structure of FT

Also, Pi coefficients are determined as $K_p = 14.2$, $K_I = 0.5$. The situation of the system is normal (faultless). Fig. 7 shows the power output by the PI controller without any fault (disturbance). The response of the turbine rotor speed with the PI controller is as Fig.8. As can be seen, the rotation speed of the rotor is converted to the desired value and has little fluctuations. The Pitch angle change of a blade is as Fig. 9. The controller (PI) used in this study works well in a normal state.

5.2. Performance Evaluation of residual generation and fault detection units in the presence of the fault

When a fault occurs, the system should switch from PI controller to FT, for this purpose FD needs to be done. Common input of the ANN model and plant (simulation setup) is the wind speed and real wind speed has been used for this purpose. A Multilayer perceptron (MLP) ANN with three inputs, hidden and output layers are used to the modeling of pitch angle. The five-minute average wind speed information, the divergences of wind speed, and

pitch angles were used for training the network using by backpropagation. If $k \geq 0$ and $i \geq 1$, $(V(n - k), e_v(n - k), \beta(n - i))$ vectors are used as input. Real wind speed collected from the MAPNA farm is sent to the simulation setup after a pre-processing. Pitch angle and power data are stored proportionally to the wind speed profile. The neural network is trained using the data produced. The number of hidden layer neurons (N), input, and output are important in such a network, the aim is to produce pitch angle, so the output neuron is 1. The appropriate values of k, i, and N should be determined in training and the optimization phase, respectively. The 25000 actual wind speed data were collected from the MAPNA farm, 15000 wind speed data of all operation ranges were used to produce pitch angle, then 10500 data were used for training, 2250 data and 2250 data were used for validation and test of network, respectively. First, the network was trained with initial values of the three important parameters.

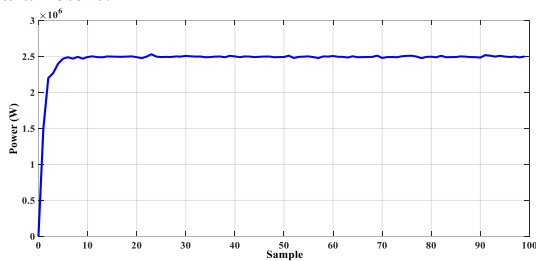


Fig. 7. Power output using the PI controller in the absence of faults and disturbance

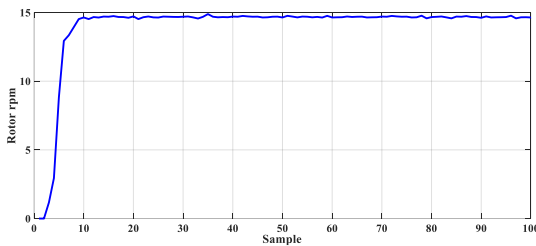


Fig. 8. The rotation speed of the rotor using the PI controller in the absence of faults and disturbance

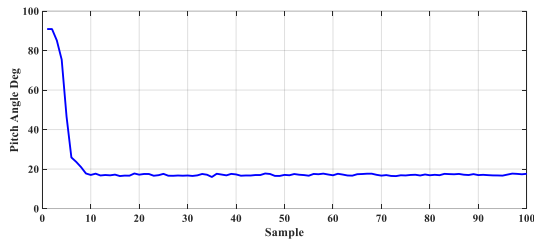


Fig. 9. Changes of the pitch angle in the absence of faults and disturbance

Then, the numbers of hidden layer neurons, step-number of past wind speed data, and its divergence and step-number of past pitch angel data were determined step by step. By taking into account the MSE criteria, $N=5$, $k=1$, and $i=1$, therefore, the number of the input vector, the number of hidden layer neurons, and the number of output vector were 6, 1, and 1, respectively. After the preparation of the ANN network, 10,000 real wind speed data were used. This data was used as shared input in the NN and plant. The performance evaluation of the plant and NN in the generation pitch angle is reflected in Fig. 10 & 11. The performance of the residual generation unit

is shown in Fig.12. To evaluate the performance of FD, a disturbance was modeled at the start of the system and randomly entered the system at $[0 \ 10] \frac{\pi}{180}$. At about 800th second, the actuator fault was seen with changes in ω_n and ξ to 7.3 and 0.75. As shown in the simulation of Fig. 13 absolute value of the normalized residual at disturbance is more than 0.5 in some times. However, it is more than 0.5 in the presence of fault which is shown by a defined threshold. In this situation, the structure acts in FT mode. In the next simulation, we eliminated the disturbance and set ω_n and ξ values to 3.42 and 0.9. Fig. 13 shows the simulation output, up to 20th seconds and in the absence of disturbance the residual is less than 0.5 and PI controller acted very well but after it and despite the actuator fault, the generated residual is more than 0.5 and FTC should be used for proper operation of the plant.

5.3. Evaluation of FTC

5.3.1. Design of system based on controller

The aim of this section is to implement the proposed FTC method on the WT's simulator. For this purpose, taking into account the system model, the implementation of this control method will be discussed.

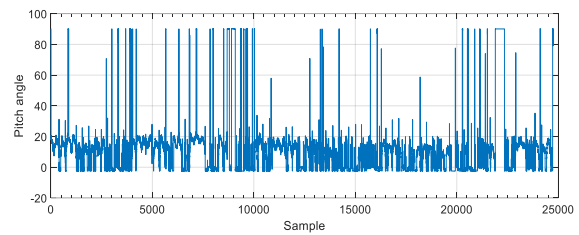


Fig. 10. Plant pitch angle output (simulator)

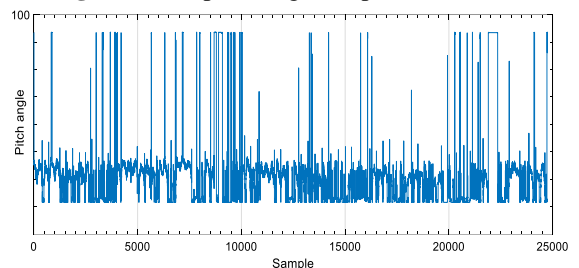


Fig. 11. ANN pitch angle output

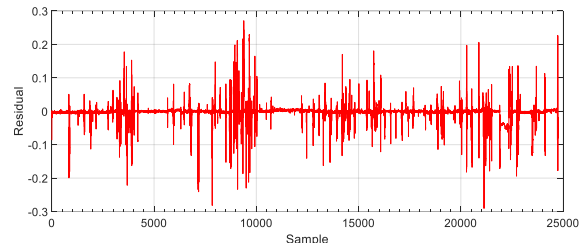


Fig. 12. Residual in the absence of actuator fault

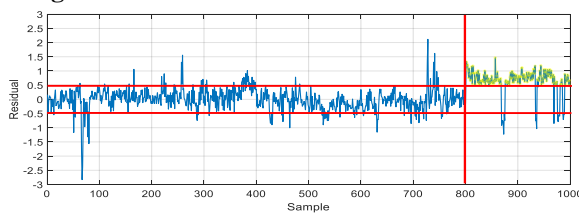


Fig. 13. Residual generated in the presence of disturbance and actuator fault

$$\begin{bmatrix} \dot{\omega}_r \\ \dot{\beta} \end{bmatrix} = \begin{bmatrix} -54.7864 & 100.5970 \\ 0 & -20 \end{bmatrix} \begin{bmatrix} \omega_r \\ \beta \end{bmatrix} + \begin{bmatrix} 0 \\ 20 \end{bmatrix} \beta_{cmd} + f(x(t)) \quad (47)$$

$$\begin{bmatrix} \dot{\omega}_{rm} \\ \dot{\beta}_m \end{bmatrix} = \begin{bmatrix} -20 & -9.7699 \\ 16 & 0 \end{bmatrix} \begin{bmatrix} \omega_{rm} \\ \beta_m \end{bmatrix} + \begin{bmatrix} 4 \\ 0 \end{bmatrix} r(t) \quad (48)$$

Where state vectors are considered as $x = [\omega_r, \beta]^T$, $f(x(t))$ and $f(x(t)) = \theta^{*T} \Phi(x(t)) + \varepsilon$. Solving the Lyapunov equation, when $Q = 2I$ and taking into account the control rule $u(t) = -K_x x(t) + K_r r(t) - \theta^T(t) \Phi(x(t))$:

$$\dot{\theta}(t) = -\Gamma \Phi(x(t)) \left[e^T(t) P - \xi \theta^T(t) \frac{d\Phi(x(t))}{dx} G^T A_m^{-1} B \right] \quad (49)$$

Where $\xi = 0.1$ and $P = \begin{bmatrix} 0.0805 & -0.0625 \\ -0.0625 & 0.2598 \end{bmatrix}$ is obtained from the Lyapunov equation and Γ as the

$$\|\Delta(t)\| \leq \left\| \begin{bmatrix} 2 & 0 \\ 0 & 2 \end{bmatrix}^{-1} \right\| \left\| \begin{bmatrix} 0.1 & \begin{bmatrix} 0.1279 & -0.1023 \\ -0.0625 & 0 \end{bmatrix} \begin{bmatrix} 2 & 0 \\ 0 & 2 \end{bmatrix} \right\| \left\| \frac{d(\theta^T(t) \frac{d\Phi(x(t))}{dx})}{dt} \right\| + \left\| \begin{bmatrix} 0.0805 & -0.0625 \\ -0.0625 & 0.2598 \end{bmatrix} \begin{bmatrix} 0 \\ 20 \end{bmatrix} \right\| \|f(x(t))\| = \quad (51)$$

$$\left\| \begin{bmatrix} 2 & 0 \\ 0 & 2 \end{bmatrix} \right\| \left\| \begin{bmatrix} 0.0256 & -0.1023 \\ -0.0625 & 0 \end{bmatrix} \right\| \left\| \frac{d(\theta^T(t) \frac{d\Phi(x(t))}{dx})}{dt} \right\| + \left\| \begin{bmatrix} -1.2500 \\ 5.1960 \end{bmatrix} \right\| 0.1745 = 2 \left[0.0343 \left\| \frac{d(\theta^T(t) \frac{d\Phi(x(t))}{dx})}{dt} \right\| + 0.9327 \right]$$

$$V(t) = e^T(t) \begin{bmatrix} 0.0805 & -0.0625 \\ -0.0625 & 0.2598 \end{bmatrix} e(t) + \text{trace} \left(\frac{1}{3024} \bar{\theta}^T(t) \bar{\theta}(t) \right) \quad (52)$$

By differentiation and after simplification, Eq.53 is obtained. Then, the stability of the studied systems with the designed controller will be discussed.

$$\begin{aligned} \dot{V}(t) &\leq -\|e(t)\| \left[2\|e(t)\| - 2 \left\| \begin{bmatrix} 0.0805 & -0.0625 \\ -0.0625 & 0.2598 \end{bmatrix} \begin{bmatrix} 0 \\ 20 \end{bmatrix} \right\| \frac{\pi}{180} \right] (10) \\ &+ 0.2 \left\| \frac{d\Phi^T(x(t))}{dx} \right\| \times \quad (53) \\ &\left\| \begin{bmatrix} 2 & 0 \\ 0 & 2 \end{bmatrix} \begin{bmatrix} 0 & 0.0625 \\ 0.1023 & -0.1279 \end{bmatrix} \begin{bmatrix} 0 \\ 20 \end{bmatrix} \right\| \|\bar{\theta}(t)\| - \|\theta_0^*\| \\ &= -\|e(t)\| \left[2\|e(t)\| - 2 \times 5.3442 \times \frac{\pi}{180} \right] (10) + 0.2 \left\| \frac{d\Phi^T(x(t))}{dx} \right\| 5.6942 \left[\|\bar{\theta}(t)\| - \|\theta_0^*\| \right] \end{aligned}$$

So $\dot{V}(t)$ will be expressed as Eq.54.

$$\dot{V}(t) \leq -c_1 [\|e(t)\| - c_2]^2 + c_3 [\|\bar{\theta}(t)\| - c_4]^2 + c_5 \quad (54)$$

Where c_1 to c_4 will be obtained as equations (55) to (58)

$$c_1 \triangleq \lambda_{\min}(Q) = \lambda_{\min} \begin{bmatrix} 2 & 0 \\ 0 & 2 \end{bmatrix} = 2 \quad (55)$$

$$c_2 \triangleq \|PB\| \varepsilon_0 / \lambda_{\min}(Q) \triangleq \left\| \begin{bmatrix} 0.0805 & -0.0625 \\ -0.0625 & 0.2598 \end{bmatrix} \begin{bmatrix} 0 \\ 20 \end{bmatrix} \right\| \frac{\pi}{180} (10) = 5.3442 \times 0.0873 = 0.4665 \quad (56)$$

$$c_3 \triangleq 0.1 \left\| \frac{d\Phi^T(x(t))}{dx} \right\| \left\| \begin{bmatrix} 2 & 0 \\ 0 & 2 \end{bmatrix} \begin{bmatrix} 0 & 0.0625 \\ 0.1023 & -0.1279 \end{bmatrix} \begin{bmatrix} 0 \\ 20 \end{bmatrix} \right\| = 0.56942 \left\| \frac{d\Phi^T(x(t))}{dx} \right\| \quad (57)$$

$$c_4 \triangleq \theta_0^* \quad (58)$$

Then the studied set will be considered as Eq.59.

$$B_r = \left\{ (e(t), \bar{\theta}(t)) \in R^n \times R^{m \times p} : 2[\|e(t)\| - 0.4665]^2 + 0.56942 \left\| \frac{d\Phi^T(x(t))}{dx} \right\| [\|\bar{\theta}(t)\| - \theta_0^*]^2 \leq c_5 \right\} \quad (59)$$

adaptive gain is 3024. Therefore, the optimal solution with a unique adaptive rule will be expressed as Eq.50.

$$\begin{aligned} \dot{\theta}(t) &= -3024 \Phi(x(t)) \left[e^T(t) \begin{bmatrix} 0.0805 & -0.0625 \\ -0.0625 & 0.2598 \end{bmatrix} - \frac{d\Phi^T(x(t))}{dx} \theta(t) \begin{bmatrix} 2 & 0 \\ 0 & 2 \end{bmatrix} \begin{bmatrix} 0 & 0.0625 \\ 0.1023 & -0.1279 \end{bmatrix} \right] \begin{bmatrix} 0 \\ 20 \end{bmatrix} \quad (50) \end{aligned}$$

5.3.2. Stability test

When $t_f \rightarrow \infty$, then $\Delta(t)$ will be calculated according to Eq.50.

That depends on modification parameter ξ and adaptive uncertainty $\|f(x(t))\|, \|\Delta(t)\|$ will be limited as long as there is uncertainty. To prove the stability of the proposed adaptive rule using the Lyapunov theorem, Lyapunov function $V(t)$ will be considered as Eq.52.

By defining r and κ and considering the equation $r = c_2 + \sqrt{c_5/c_1}$ and $\kappa = c_4 + \sqrt{c_5/c_3}$, the adaptive rule is stable at out of B_r range. In other words $\dot{V}(t) \leq 0$

$$\rho = \sqrt{\frac{0.3237r^2 + 3.306 \times 10^{-4} \kappa^2}{0.0003}} \quad (60)$$

$$\text{Where } \bar{P} = \begin{bmatrix} 0.0805 & -0.0625 & 0 \\ -0.0625 & 0.2598 & 0 \\ 0 & 0 & 3.306 \times 10^{-4} \end{bmatrix}.$$

To prove this range, Ω_α and α considered as $\Omega_\alpha = \{q(t) \in B_r : q^T(t) \bar{P} q(t) \leq \alpha\}$ and $\alpha = \min_{\|q(t)\|=r} q^T(t) \bar{P} q(t) = 0.0003r^2$.

Since $V(t)$ is defined as $V(t) = q^T(t) \bar{P} q(t) = e^T(t) P e(t) + \text{trace} [\bar{\theta}^T \Gamma^{-1} \bar{\theta}]$ and Ω_α is an invariant set with the length of $\alpha \geq 0.3237r^2 + 3.306 \times 10^{-4} \kappa^2$ then the least size of B_r is estimated by Eq.60.

5.3.3. Simulation and comparison with other methods

In this section, the FTC method (ORMRAC) performance is investigated, as mentioned earlier in the real plant it is not possible to change the controller, but to do a simulation in the simulator, PI is replaced by ORMRAC and a thorough investigation is carried out on its performance. The proposed method improves the MRAC method, in simulations MRAC method is compared with ORMRAC. Simulations are done only in the third area of operation. In this system, the disturbance is modeled as $[0 \ 10] \frac{\pi}{180}$, the results of a simulation with the FTC controller in the presence of disturbance are obtained from figures 14 to 19. By examining the figures, it was observed that the controller can control the pitch system of WT at the presence of disturbance. Fig. 14 shows the power output. According to the figure it was seen that, despite the disturbance, the ORMRAC controller was able to maintain power output at about 2.5 MW. Although the MRAC method in the presence of disturbance has better performance than the PI controller but the performance of ORMRAC is clearly better. Fig. 15 shows the rotor speed changes. According to this figure, the ORMRAC controller despite the disturbance

could keep the rotor speed at a nominal rate. Fig. 16 shows the change in the pitch angle, the goal is to achieve the power of 2.5 MW. To evaluate the proposed method in this section of the controller error in the presence of disturbance will be discussed. Fig. 17 shows the output power error of the controllers. As can be seen, changes with ORM-RAC are centered on zero. Fig.18 shows the rotor speed error. According to figures 19 and 20 as well as Table II, ORM-RAC performance can be compared with the MRAC. It can be seen that the error parameters of the controller are highly desirable. Control parameters of the ORM-RAC method are compared to MRAC. The results are shown in Table III. According to the table, it is clear that the overshoot of power output is 2.7668. This parameter is 0.0902 in the speed of the rotor. In the proposed method, the gain of adaptive control is high, since there is a direct relationship between controls gains with adaptation speed, but the high adaptive gain results in instability, therefore the gain value cannot be increased to the desired value in the use of any controller. The adaptive control gain for the ORM-RAC method is 3024. The speed of adaptation of this method is also desired. Tables IV and 5 are provided for a better comparison of ORM-RAC with the MRAC method. In Table IV in both methods, the adaptive gain is fixed and equals to 2800. The modification factor gain is 0.1. According to the table, we see that both in power output of the turbine and rotor speed, the overshoot in the

proposed method is better than the MRAC and the rise time is less. To compare these two methods in Table V, the overshoot of output power and rotor speed were fixed to 1.1067 and 0.0902 respectively. Also taking into account the modification factor gain of 0.1, the adaptive gain and rise time in power output and rotor speed is evaluated using two controllers. According to the table, it can be seen that at the output power with the same overshoot, the adaptive gain is higher in the proposed method compared to the MRAC method as a result of the rise time is better. This can be concluded from rotor speed as well. Table VI provides a comparison of the proposed method with some other articles.

6. Implementation of the proposed structure

The actual wind speed from the MAPNA farm is given as input to the setup. Data includes all the different operational areas of the WT.

In the first scenario, ω_n and ξ parameters are changed to 5.93 and 0.45 and the performance of the proposed structure was simulated with and without ORM-RAC. The fault occurs at 1000th seconds. As shown in Fig. 21 from the power signal and rotor speed signal, amplitude of the signal at the absence of FT is higher than the other two modes. The output signal at the presence of the FT is closer to fault-free. The fault is well compensated by ORM-RAC. However, it can be seen that the residual signal is higher than 0.5 and the FT switch is active.

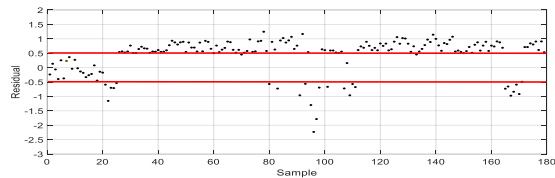


Fig. 14. Residual generated in the presence of disturbance and actuator fault

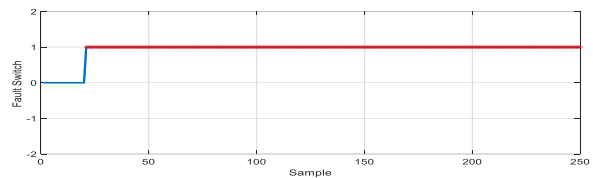


Fig. 15. The performance of the fault indicator switch

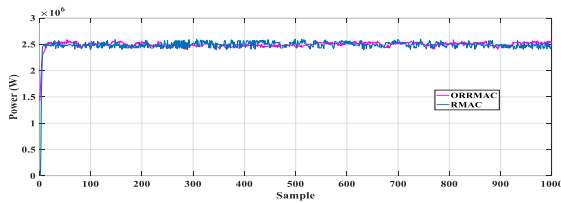


Fig. 16. WT output power

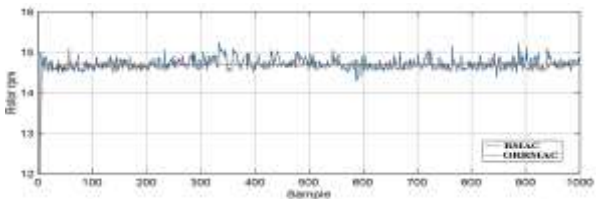


Fig. 17. The speed of the rotor using the MRAC and ORM-RAC

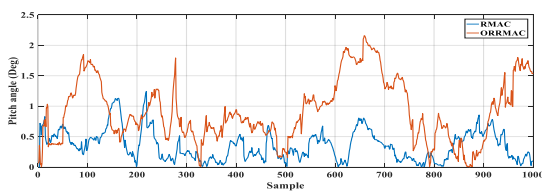


Fig. 18. Changes in the pitch - angle of WT using ORM-RAC and MRAC in the presence of disturbance

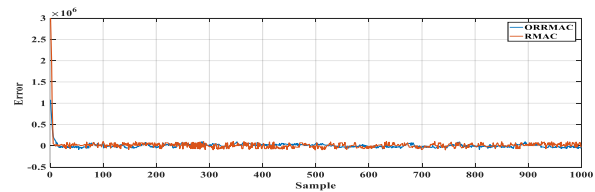


Fig. 19. WT power output tracking error using ORM-RAC and MRAC

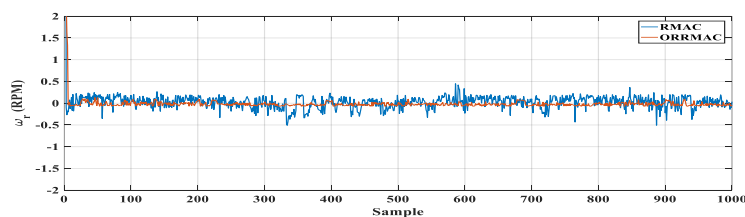


Fig. 20. Tracking error of rotor speed using MRAC and ORM-RAC

Table II. Compares the error criteria of MRAC and ORMRAC

		Rotor speed (r.p.m)	Power (MW)
Maximum of error	ORMRAC	0.431	0.2400
	MRAC	0.132	0.3000
Minimum of error	ORMRAC	0.0700	0.1039
	MRAC	0.0400	0.1000
Variance of error	ORMRAC	0.0276	0.0123
	MRAC	0.1203	0.1008
The standard deviation of error	ORMRAC	0.1661	0.1391
	MRAC	0.3469	0.1490
Root Mean Square Error	ORMRAC	0.1664	0.1393
	MRAC	0.3483	0.1498

Table III. Comparison of the control parameters for MRAC and ORMRAC

	Γ	Parameters	Rise time	Overshoot	Maximum value	Time of maximum value
ORMRAC	3024	Output power	4.5325	1.1067	2.6000e+6	499
		Rotor speed	3.2513	0.0902	14.763	384
MRAC	3024	Output power	10.5573	1.8145	2.6940e+6	54
		Rotor speed	4.1541	0.3093	15.34	816

Table IV. Comparison of the two proposed controller at the fixed adaptive gain of 2800 and gain modification factor of 0.1

		Parameters	Rise time	Overshoot
MRAC	Output power	10.9180	1.7961	
	Rotor speed	4.5071	0.3022	
ORMRAC	Output power	6.0271	0.8725	
	Rotor speed	4.6817	0.0798	

Table V. Comparison of the two controllers at fixed power overshoot of 1.10671 and rotor speed of 0.0902 and modification factor gain of 0.01

		Parameters	Adaptive gain	Rise time
MRAC	Output power	2627	12.4913	
	Rotor speed	1921	9.2314	
ORMRAC	Output power	3024	4.5325	
	Rotor speed	3024	3.2513	

Table VI. Comparison of ORMRAC method with other methods

Ref	[10]	[43]	[11]	[12]	[13]	[14]	[15]	This wok
T. S	NL	NL	NL	NL	NL	NL	NL	NL
C. S	LI	LI	LI	LI	LI	LI	LI	LI
G. T	DFIG	DFIG	DFIG	DFIG	PMSG	DFIG	DFIG	DFIG
O.A	3	all	3	3	2	3	3	all
A.W.S	-	11.4	18	18	12.5	18	11.3	12.43
N.P	2	5.5	5	5	-	-	5	2.5
T.N.V	9	30	10	-	-	-	17	6
P.O	1.075	0	-	0.1	-	-	1.1	1.1064
P.A	-	≈0.57	-	-	-	1.1	≈1.1833	0.3505
P.A.M	-	-	2.781	0.6081	-	-	-	-
A.N.O.P	≈1.09	≈ 0.782	0.9996	-	≈ 0.871	1.01	-	0.99352
A.N.R.S	-	-	-	-	≈ 0.812	-	-	0.9995
A.N.G.S	-	-	-	-	-	0.85	0.9962	-
R.S.E	-	-	0.042	0.1067	0.8886	-	-	0.1203
P.O.E	-	-	0.00415	0.2063	-	-	-	0.1498
G.S.E	-	-	-	-	-	0.06	0.0413	-

Ref: Reference/ T. S: Turbine Structure/ C.S: Controller Structure/ G.T: Generator Type / O.A: Operation Area/ A.W.S: Average wind speed/ N.P: Nominal Power/ T.N.V: Time to be the nominal value/ P.O: Power Overshot/ P. A: Pitch Angle/ P.A.M: Pitch-angle Matching error (degrees)/ A.N.O.P: Average normalized output power rate/ A.N.R.S: Average normalized rotor speed rate/ A.N.G.S: Average normalized generator speed rate/ R.S.E: Rotor speed error (r.p.m)/ P.O.E: Power output error (M.W)/ G.S.E: Generator speed error (r.p.m). LI: Linear/ NL: Noun Linear

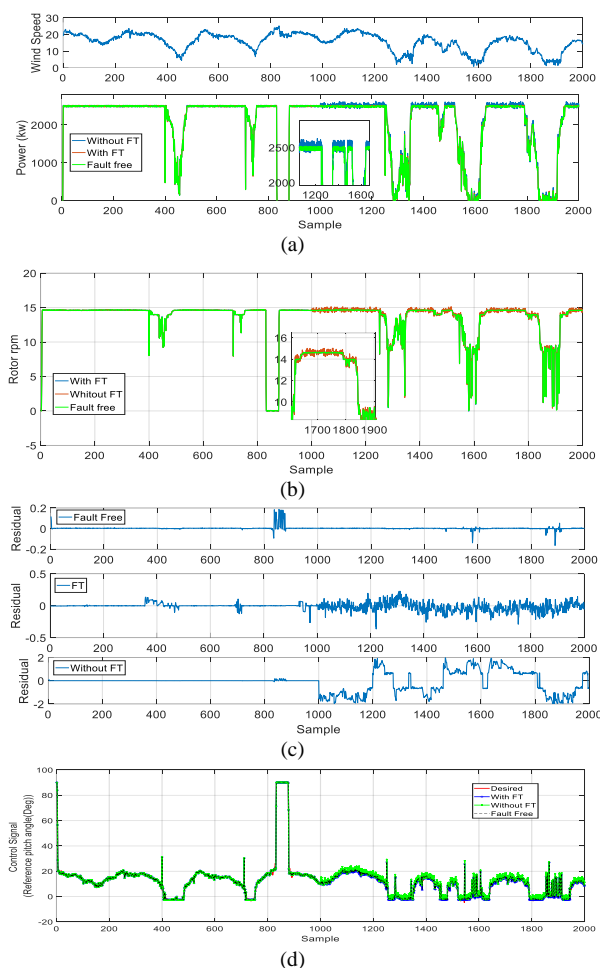


Fig. 21. Performance of the proposed structure, (a): Power signal with $\omega_n = 5.93$ and $\xi = 0.45$, (b): Rotor speed signal with $\omega_n = 5.93$ and $\xi = 0.45$, (c): Residual signal with $\omega_n = 5.93$ and $\xi = 0.45$, (d) control signal

7. Conclusion

In this paper, a new FTC method is proposed to fault compensates and deals with the disturbance. The conventional MRAC method was improved and optimality and robustness were added to it. ORMRA method acts in the control loop when the actuator fault occurs. The method acts without prior knowledge about the disturbance/fault. A software simulator based on Simulink/MATLAB was used to verify the proposed method based on WT practical data. ANN was used for residue generation. The ORMRA methods were evaluated exactly and it was demonstrated that tracking error of power tracking and rotor rotation speeds is very low. Thus ORMRA methods can be used to maintain power generation in the event of fault and disturbance.

References

- [1] A. Dameshghi, M.H. Refan, "A new strategy for short-term power-curve prediction of wind turbine based on PSO-LS-WSVM", *IJEEE*, vol. 14, no. 4, pp. 392-403, 2018.
- [2] M. Rahimi, M.R. Esmaceli, "Power controller design and damping improvement of torsional oscillations in the 710 kW DFIG based wind turbine installed at the Binalood site," *Tabriz Journal of*

Electrical Engineering, vol. 46, no. 4, pp. 123-134, 2 (In persian).

- [3] A. Dameshghi, M.H. Refan, P. Amiri, "Wind turbine doubly fed induction generator rotor electrical asymmetry detection based on an adaptive least mean squares filtering of wavelet transform", *Wind Engineering*, vol. 10, no. 3, pp. 11-22, 2019.
- [4] A. Dameshghi, M.H. Refan, "Combination of condition monitoring and prognosis systems based on current measurement and PSO-LS-SVM method for wind turbine DFIGs with rotor electrical asymmetry", *Energy Systems*, pp. 1-30, 2019.
- [5] Z. Jiang, M. Karimirad, T. Moan, "Dynamic response analysis of wind turbines under blade pitch system fault, grid loss, and shutdown events", *Wind Energy*, vol. 17, no. 9, pp. 1385-1409, 2014.
- [6] Y. Shabboei, A. Rikhtegari, S. Khanmohammadi, "Design of Fault Tolerant Nonsingular Terminal Sliding Mode Control for Nonlinear Systems based on an Adaptive Extended Kalman Filter," vol. 46, no. 4, pp. 173-183, 2016 (In persian).
- [7] H. Schulte, E. Gauterin, "Fault-tolerant control of wind turbines with hydrostatic transmission using Takagi-Sugeno and sliding mode techniques", *Annual Reviews in Control*, vol. 40, pp. 82-92, 2015.
- [8] J. Lan, R. J. Patton, X. Zhu, "Fault-tolerant wind turbine pitch control using adaptive sliding mode estimation", *Renewable Energy*, vol. 116, pp. 219-231, 2018.
- [9] H. Badihi, Y. Zhang, H. Hong, "Fault-tolerant cooperative control in an offshore wind farm using model-free and model-based fault detection and diagnosis approaches", *Appl Energ*, vol. 201, pp. 284-307, 2016.
- [10] L. Jalali, M. R. Nezhad-Ahmadi, M. Gohari, P. Bigelow, S. McColl, "The impact of psychological factors on self-reported sleep disturbance among people living in the vicinity of wind turbines", *Environmental Research*, vol. 148, pp. 401-410, 2016.
- [11] H. Badihi, Y. Zhang, H. Hong, "Model-based Active Fault-tolerant Cooperative Control in an Offshore Wind Farm", *Energy Procedia*, vol. 103, pp. 46-51, 2016.
- [12] E. B. Muhando, T. Senjyu, A. Uehara, "Gain-Scheduled H_∞ Control for WECS via LMI Techniques and Parametrically Dependent Feedback Part II: Controller Design and Implementation", *IEEE T IND ELECTRON*, vol. 58, no. 1, pp. 57-68, 2010.
- [13] M. Mirzaei, H. H. Niemann, N. K. Poulsen, "A μ -synthesis approach to robust control of a wind turbine", *50th IEEE Conference on Decision and Control and European Control Conference (CDC-ECC)*, 2011, Orlando, FL.
- [14] M. Mirzaei, M. Soltani, K. Poulsen, H. H. Niemann, "An MPC approach to individual pitch control of wind turbines using uncertain LIDAR measurements", *European Control Conference (ECC)*, Zurich INSPEC, 2013. Accession Number: 13950748.
- [15] M. L. Corradini, G. Ippoliti, G. Orlando, "Robust Control of Variable-Speed Wind Turbines Based on an Aerodynamic Torque Observer", *IEEE T CONTR SYST T*, vol. 21, no. 4, pp. 1199-1206, 2013.
- [16] L. Danyong, S. Yongduan, C. Wenchuan, H. Karimi, "Wind Turbine Pitch Control and Load

- Mitigation Using an L1 Adaptive Approach”, *Mathematical Problems in Engineering*, 2014.
- [17] D. Corcuera, A. Pujana, A. Ezquerro, M. Seguro, E. Landaluze, “ H_{∞} Based Control for Load Mitigation in Wind Turbines”, *Energies*, vol. 5, no. 4, pp. 938-967, 2012.
- [18] L. L. Fan, Y. D. Song, “Neuro-Adaptive Model-Reference Fault-Tolerant Control with Application to Wind Turbines”, *IET Control Theory & Applications*, vol. 6, no. 4, pp. 475-486, 2012.
- [19] E. Kamal, A. Aitouche, R. Ghorbani, M. Bayart, “Robust Fuzzy Fault-Tolerant Control of Wind Energy Conversion Systems subject to Sensor Faults”, *IEEE Transactions on Sustainable Energy*, vol. 3, no. 2, pp. 231-241, 2012.
- [20] C. Sloth, T. Esbensen, J. Stoustrup, “Robust and Fault-Tolerant Linear Parameter-Varying Control of Wind Turbines”, *Mechatronics*, vol. 21, no. 4, pp. 645-659, 2011.
- [21] H. Badihi, Y. M. Zhang, H. Hong, “Fuzzy Gain-Scheduled Active Fault-Tolerant Control of a Wind Turbine”, *J FRANKLIN I*, vol. 351, no. 7, pp. 3677-3706, 2014.
- [22] S. Simani, P. Castaldi, “Data-Drive Design of Fuzzy Logic Fault Tolerant Control for a Wind Turbine Benchmark”, *IFAC Proceedings*, vol. 45, no. 20, pp. 108-113, 2012.
- [23] S. Simani, S. Farsoni, P. Castaldi, “Fault-Tolerant Control of an Offshore Wind Farm via Fuzzy Modelling and Identification”, *IFAC-Papers OnLine*, vol. 48, no. 21, pp. 1345-1350, 2015.
- [24] H. Badihi, Y. Zhang, H. Hong, “Model Reference Adaptive Fault-Tolerant Control for a Wind Turbine against Actuator Faults”, *Conference on Control and Fault-Tolerant Systems (SysTol)*, October 2013 Nice, France.
- [25] Y. Vidal, Ch. Tutivén, J. Rodellar, L. Acho, “Fault Diagnosis and Fault-Tolerant Control of Wind Turbines via a Discrete Time Controller with a Disturbance Compensator”, *Energies*, vol. 8, no. 5, pp. 4300-4316, 2015.
- [26] F. Shi, R. Patton, “An active fault tolerant control approach to an offshore wind turbine model”, *Renewable Energy*, vol. 75, pp. 788-798, 2014.
- [27] S. Cho, Z. Gao, T. Moan, “Model-based fault detection, fault isolation and fault-tolerant control of a blade pitch system in floating wind turbines”, *Renewable Energy*, vol. 120, pp. 306-321, 2018.
- [28] H. Badihi, Y. Zhang, S. Rakheja, P. Pillay, “Model-Based Fault-Tolerant Pitch Control of an Offshore Wind Turbine”, *IFAC-PapersOnLine*, vol. 51, no. 18, pp. 221-226, 2018.
- [29] H. Badihi, Y. Zhang, “Fault-tolerant individual pitch control of a wind turbine with actuator faults”, *IFAC-PapersOnLine*, vol. 51, no. 24, pp. 1133-1140, 2018.
- [30] J. Lan, R. J. Patton, X. Zhu, “Fault-tolerant wind turbine pitch control using adaptive sliding mode estimation”, *Renewable Energy*, vol. 116, pp. 219-231, 2018.
- [31] Y. Liu, R. J. Patton, J. Lan, J. “Fault-tolerant Individual Pitch Control using Adaptive Sliding Mode Observer”, *IFAC-PapersOnLine*, vol. 51, no. 24, pp. 1127-1132, 2018.
- [32] S. Mullick, “Design of Model Reference Adaptive Controller with Multiplicative Structured Uncertainty”, *Msc Thesis, Jadavpur University*, 2012.
- [33] J. Nelson, M. J Balas, R. S Erwin, “Model Reference Adaptive Control of Mildly Non-Linear Systems with Time Varying Input Delays – Part I”, *Advances in Aerospace Guidance, Navigation and Control*, 2013.
- [34] K.S Narendra, M. Annaswamy, “A new adaptive law for robust adaptation without persistent excitation”, *IEEE T AUTOMAT CONTR*, vol. 32, no. 2, pp. 134-145, 1987.
- [35] T. Nguyen, “Optimal control modification for robust adaptive control with large adaptive gain”, *Syst Control Lett*, vol. 61, no. 4, pp. 485-494, 2012.
- [36] T. Zhang, S. S Ge, C. C. Hang, “Adaptive control of first-order systems with nonlinear parameterization”, *IEEE T AUTOMAT CONTR*, vol. 45, no. 8, pp. 1512-1516, 2000.
- [37] P.A. Ioannou, V. Kokotovic, “Instability analysis and improvement of robustness of adaptive control”, *Automatica*, vol. 20, no. 5, pp. 583-594, 1984.
- [38] K. Khalil, J. W. Grizzle, “Nonlinear systems,” vol. 3. New Jersey: Prentice hall, 1996.
- [39] G. Cybenko, “Approximation by superpositions of a sigmoidal function”, *MCSS*, vol. 2, no. 4, pp. 303-314, 1989.
- [40] C.A. Micchelli, “Interpolation of scattered data: distance matrices and conditionally positive definite functions”, *Constructive Approximation*, vol. 2, no. 1, pp. 11-22, 1986.
- [41] A.J. Calise, T. Yucelen, “Adaptive Loop Transfer Recovery”, *JGCD*, vol. 35, no. 3, pp. 807-815, 2012.
- [42] Mapna 2.5 MW (Mapna Group) Wind Turbine available at http://www.thewindpower.net/turbine_en_986_mapna-group_2500.php
- [43] F. A. Inthamoussou, F. B Bianchi, R. J. Mantz, “LPV Wind Turbine Control with Anti-Windup Features Covering the Complete Wind Speed Range”, *IEEE T Energy Conver*, vol. 29, no.1, pp. 259-266, 2014.